Improved recovery of carboxylic acids using sequential cationic-anionic adsorption steps: A highly competitive ion-equilibrium model

Improved recovery of carboxylic acids using sequential cationic-anionic adsorption steps: *a highly competitive ion-equilibrium model*

Sarah Notarfrancesco[1‡], Elena Morselli[1‡], Gonzalo A. Martinez[1]*, Weronica Harasimiuk [2], Joana M. B. Domingos[1], Andrea Negroni[1], Fabio Fava[1], Lorenzo Bertin[1]

[1]Department of Civil, Chemical, Environmental and Materials Engineering (DICAM), University of Bologna, via Terracini, 28, I-40131 Bologna, Italy

[2] Institute of Food Technology and Analysis, Lodz University of Technology, Stefanowskiego 4/10, 90-924 Lodz, Poland

[‡] These authors equally contributed to the manuscript.

Sarah Notarfrancesco: sarah.notarfrancesc2@unibo.it
Elena Morselli: elena.morselli4@unibo.it
Gonzalo A. Martinez (*corresponding author): gonzalo.martinez3@unibo.it
Tel: (+39) 051 20 90314
Weronica Harasimiuk: w.harasimiuk@gmail.com
Joana M. B. Domingos: joana.bendada@unibo.it
Andrea Negroni: andrea.negroni4@unibo.it
Fabio Fava: fabio.fava@unibo.it
Lorenzo Bertin: lorenzo.bertin@unibo.it

ABSTRACT

A strong cationic resin (Lewatit-S2568H) was used to pre-treat four actual broths rich in carboxylic acids (CAs) to obtain free Na^+ streams (final pH 1.5-2.4). Thereafter, three weak anionic resins (AnRes) were compared for the recovery of CAs by performing multicomponent batch adsorption tests using one of the pre-treated broths. Subsequently, further multicomponent adsorption tests were performed using the other three broths and the most performant AnRes (Lewatit-A365). This allowed to define adsorption isotherm profiles of CAs, Cl^-, phosphates and other organic compounds (COD_{Other}) for each broth. Besides confirming anions competition for resin exchange sites, results also evidenced that Na^+ competed with the AnRes exchange sites for binding the CAs, while COD_{Other} exerted a negligible competition for CA adsorption. A homogeneous mass action ideal model, that also considers Na^+ competition, was calibrated using the collected data. It shows a very good capability to predict adsorption isotherms despite very dissimilar broths were used.

KEYWORDS

Volatile fatty acids; Organic fraction of municipal solid waste; Grape pomace; Fruit and vegetable waste; Ion exchange resin; Agro-industrial by-product valorisation

ABBREVIATIONS

AnRes anionic resins
CAs carboxylic acids
CatRes cationic resin
COD chemical oxygen demand
COD_{CAs} COD related to the CAs content
COD_{Cl} COD related to Cl^- content
COD_{Meas} COD measured

COD_{Other} COD related to other organic compounds

EU European Union

FVWs fruit-and-vegetable by-products

GP grape pomace

ISE ion-selective electrodes

PO_4^{x-} phosphates, all species

PHAs polyhydroxyalkanoates

UBWs urban biowaste

1. INTRODUCTION

The demand for added value chemicals on the one hand and the need to manage and valorise wastes or by-products on the other hand, are two of the most prominent concerns worldwide about circular economy. In such a framework, stands the chance of coupling organic matter valorisation with the biotechnological production of carboxylic acids (CAs). In fact, CAs can be produced by a simple and economic anaerobic acidogenic fermentation process carried out by mixed microbial cultures. Among the numerous applications, CAs can be employed as precursors of valuable molecules such as esters, ketones and polyhydroxyalkanoates (PHAs), among others [1,2].

In this context, urban biowaste (UBWs) valorisation has been recently studied by Majone and co-workers for instance [3]. The proposed valorisation scheme includes the anaerobic fermentation of concentrated sewage sludge and the organic fraction of municipal solid waste. CAs were then used as substrate to produce PHAs by employing a mixed microbial culture system [4]. The parallel esterification of part of the produced CAs has been explored alongside since it would allow obtaining further added value products which in turn can also be used for PHAs extraction and purification. To this end, CAs must be separated from the aqueous fermentation broth before esterification: being water a by-product of esterification

reaction, CA recovery in an organic solvent (e.g. ethanol) would move the esterification equilibrium to the products, this resulting in enhanced reaction yields [5].

Anion exchange resins can serve for the selective adsorption of CAs from wastewaters or from fermentation broths [6–8]. Rodriguez et al. reported an innovative desorption technology but using a strong anionic resin, which has low exchange capacity, thus limiting final CA concentration in the desorbed stream. Weak anionic resins, with high exchange capacity, were employed in the other two works. Uslu et al. proved the potentiality of the weak anionic resin by utilizing laboratory prepared CA solutions, hence results need to be validated by using actual CA-rich streams. Interestingly, Rebecchi et al. described CA recovery from actual broth obtained from the acidogenic fermentation of grape pomace (GP). However, under the explored most favourable pH (i.e. promoting resin functional groups protonation), the overall CA adsorption yield was low (about 30%), this compromising the process economic feasibility. As a whole, the proposed strategy is affected by the fact that CA-rich broths are usually close to neutral pH (5<pH<7), this meaning that each mole of carboxylate is paired with a cation (e.g. Na^+) arising from the base (e.g. NaOH) added during the fermentation to adjust the pH level. Thus, carboxylates are less available for ionic adsorption due to the formation of ion pairs in the solution ($R\text{-}COO^- Na^+$) [9]. This is in accordance with the fact that a NaOH solution is usually applied for desorbing the anions from the resin in an almost stoichiometric relation [8]. Overall, the recovery of CAs using anionic resins depends on the occurrence and interference of all inorganic ions, which must be also considered for modelling adsorption isotherms using mass-action law. Among anions, phosphates (all species, here on called PO_4^{x-}) and chloride (Cl^-) are competitors for exchange sites on the anion resin [10,11].

The present work is aimed to maximize CA extraction from actual fermentation broths by coupling a cation adsorption step with a consecutive anion adsorption stage, as shown in the graphical abstract. This would allow to remove Na^+, rendering $R\text{-}COO^-$ free and available for anion resin exchange. Gonzalez *et al.* applied the same strategy but for the adsorption of inorganic anions rather than the main product (lactic

acid) [12] and a related patent describing the strategy was registered later on [13]. More recently, a similar approach was reported for the adsorption and recovery of D-lactic acid from an actual fermentation broth based on dried distiller's grains with soluble hydrolysates [14]. However, none of these works reported overall ion equilibrium models. Zaini et al [14] just applied pure empirical models (having poor extrapolation ability), while the homogeneous ideal model assessed in the previously mentioned work using GP [8] does not include the competitive effects of Cl^-, PO_4^{x-} and Na^+ already occurring in the actual broth, while only the added Cl^-/Na^+ (HCl/NaOH) and carbonates (unlikely present at the reported concentrations) were considered as interferents. On the other hand, many authors have developed ideal and non-ideal homogeneous mass action models, but few of them were validated/calibrated using actual process streams [15,16]. Indeed, a simplified homogeneous model reflecting anions and cations competitions and validated using actual CA-rich broths has never been proposed.

With all this in mind, the specific aims of this study were: *a)* to verify the exchange capacities of cationic (for Na^+ and NH_4^+) and anionic (for CAs, Cl^- and PO_4^{x-}) resins; *b)* to pre-treat four actual broths using the cationic resin and evaluate the step performance*; c)* to select the most suitable anionic resin among the tested ones containing tertiary amine or bifunctional groups; *d)* to verify the feasibility of applying the simple desorption procedure reported elsewhere [8]; *e)* to propose a simplified ionic equilibrium model (mass action) capable of predicting the total CA concentrations (in the resin and in the liquid phases) by measuring uniquely the pH at the equilibrium; and *f)* to calibrate and asses the model by using four diverse actual CA-rich broths with significantly different ions and matrix compositions, deriving from the acidogenic fermentation of two diverse UBWs (UBW1 and UBW2), fruit-and-vegetable by-products (FVWs) and a red grape pomace (GP).

The avant-garde employment of four very dissimilar actual broths allowed progressing beyond the state of art by *(1)* demonstrating the effectiveness of a cation-exchange pre-treatment which would enable to

recover almost 100% of the CAs occurring in broths by using an anionic resin with high exchange capacity, *(2)* developing a semi empirical homogeneous mass action ideal model that considers the interferences of the inorganic ions (Cl^-, PO_4^{x-} and Na^+ occurring in the broths) on CA adsorption, *(3)* demonstrating that interfering effects due to the occurrence of other non-identified organic compounds are negligible, and *(4)* highlighting that Na^+ competition rather than resin's functional-group protonation is a major concern for recovering CAs from actual broths using anionic resins.

2. MATERIAL AND METHODS

2.1. Resins, reagents and acidogenic effluents

The strong cationic resin (CatRes) Lewatit-S2568H, with sulfonic acid functional group in the H^+ form, was used to pre-treat the four actual broths. To evaluate the role of the solid phase in CA recovery, three anionic resins (AnRes) were preliminary selected according to their nominal exchange capacity and a previous experience [8], namely (brand, functional groups, nominal exchange capacity in eq/L): Amberlyst A21 (DoW, tertiary amine, 1.3), Lewatit S4528 (Lanxess, tertiary amine, 1.7) and Lewatit A365 (Lanxess, tertiary and quaternary amines, 3.4). Main chemical-physical characteristics of all resins are reported in Sup. Material Table S1. All Lewatit resins were kindly provided by Lanxess-Italy, while Amberlyst A21 and all the required reagents were purchased from Merck.

The two fermented UBWs (UBWs1 and UBWs2) used in the study were provided by an external research group in the framework of the ResUrbis EU project [3]. UBWs1 and UBWs2 were generated in different batches carried out with a pilot acidogenic fermenter located at the wastewater treatment plant of Treviso, thus with similar ions (Na^+, NH_4^+, CAs, Cl^- and PO_4^{x-}) and other organic matter (COD_{Other}) composition. The FVWs and GP were kindly provided by Biosphere S.R.L and Caviro Extra S.p.A companies, respectively. Both by-products were stored at 6 °C for less than 4 days before processing.

FVWs and GP were anaerobically fermented in 1 L Pyrex bottles under batch conditions (pH 7, 37 °C, 150 rpm) until constant CA concentration was achieved (7-10 days), according to the procedures reported elsewhere [17]. All four actual broths were processed for suspended solids removal according the procedure conducted by the PHA pilot plant described elsewhere [4]; in details, the effluents were centrifuged and filtered at 0.2 µm (cellulose acetate syringe filters were used instead of the ceramic module used at pilot scale) before use. In the present work they were stored at 4 °C until use. CA compositions in the actual broths were mainly (on % molar bases): acetic (58-69), propionic (2-8), butyric (20-25), valeric (0-5) and hexanoic (1-8) acids. Main chemical features of these target broths are reported in **Table 1** (UBWs1-*pre*, UBWs2-*pre*, FVWs-*pre* and GP-*pre*).

2.2. Experimental approach

All resins were conditioned according to the suppliers' procedures. Different sets of batch experiments (20-22 conditions each) were conducted for defining single and multi-component adsorption isotherms (25°C and 150 rpm). Each experimental point (20-22 points per isotherm) was accomplished by loading a 10 mL glass vial with 0.05 to 1.20 g of resin (dry weight) and 2 mL of liquid (i.e. water solutions or actual broth). Total volumes in each container were accurately measured by weighting the empty vials as well as the added amounts of resin and liquids. Isotherms experiments were stopped after 120 min, according to dedicated preliminary single-condition tests executed using online continuous pH measurements in a 10 mL vial (Sup. Material, Section S2.1). At the end of the isotherm-tests, the liquid was separated by means of a syringe, pH was measured and the concentrations of target analytes at the equilibrium were determined, namely: $[NH_4^+]_{Eq}$, $[Na^+]_{Eq}$, total CAs ($[CAs]_{Eq}$), $[Cl^-]_{Eq}$, $[PO_4^{x-}]_{Eq}$ and $[COD_{Other}]_{Eq}$ (calculated as reported in **Section 2.5**).

The adsorbed concentrations for each target chemical (q_n, mol/g dry resin) were calculated as follows:

$$q_n = \frac{(C_0.V_{Sample} - C_{Eq}.V_{Tot})}{m_{res}} \quad (1)$$

where C_0 and C_{Eq} represent the initial and equilibrium liquid concentrations of NH_4^+, Na^+, CAs, Cl^- or PO_4^{x-}, V_{Sample} the volume of added broth or lab-prepared solution, V_{Tot} the total liquid of the system (i.e. V_{Sample} plus the water already contained in the activated resins), and m_{res} is the resin dry mass.

2.2.1. Resins characterisation

All resins were characterised, in terms of exchange capacity and affinity with target ions, by determining single component adsorption isotherms as mentioned above. NH_4^+ and Na^+ isotherms were defined by using ammonium acetate and sodium acetate water solutions (ca. 0.1 M). For the three AnRes, acetic acid (0.5 M), HCl (0.5 M) and H_3PO_4 (0.35 M) water solutions were separately used to define CAs, Cl^- and PO_4^{x-} adsorption isotherms. Langmuir $\left(q = q_{max}.C_{Eq}/\left(K_s + C_{Eq}\right)\right)$ and Freundlich ($q = k.{C_{Eq}}^n$) models were used to fit CatRes and AnRes obtained results [18]. Specifically, the linearized form of the equations and the correlation coefficient (R^2) were used to evaluate the fittings.

2.2.2. Actual broth pre-treatments with the cationic resin

In order to remove cations, UBWs1, FVWs and GP actual broths were separately pre-treated with the CatRes Lewatit S2568H by flowing them through a 60 mL syringe packed with 14.5 g of CatRes (dry bases). First portions (ca. 40 mL) of cation-free effluents were discarded as they resulted diluted with the water contained in the activated-CatRes. Importantly, broths' pH diminishes due to cations removal. Thus, the following portions were collected until the resulting pH of the accumulated liquid was 1.51-2.50 (**Table *1***). Then, the CatRes was regenerated by sequentially manually flowing (ca. 1-2 mL/min): *(i)* 40 mL of deionised water, *(ii)* 140 mL of HCl 6%, and *(iii)* 175 mL of deionised water. Subsequently, a new adsorption-desorption cycle was carried out. Each broth required about two cycles for obtaining ca. 350 mL of treated liquid to be used in the AnRes experiments. However, without carrying out a proper

breakthrough test, the mentioned pre-treatment cycles did not allow calculating the resin exchange capacity.

Differently, UBWs2 was pre-treated using a pilot scale column (133 cm high and 2.7 cm diameter), packed with the same CatRes (bed height 77 cm). Five adsorption-desorption cycles were carried out, with the adsorption step performed and monitored as breakthrough test. First flowed portions (ca. 600 mL) were discarded as described above, while the consecutive portions were collected until the resulting pH of the accumulated liquid was 1.46. Subsequently, the effluent reservoir was replaced and the adsorption was conducted until AnRes saturation. Total exchange capacities were calculated by material balance. Then, the CatRes was regenerated by sequentially flowing (ca. 34 mL/min): *(i)* 0.6 L of deionised water, *(ii)* 2 L of HCl 6%, and *(iii)* 2.5 L of deionised water. Pilot column pre-treatment allowed to obtain an effluent portion almost completely deprived of cations (having the lowest pH tested in this work for CA extraction) and with the same concentration of CAs originally present in UBWs2 (**Table 1**).

2.2.3. Selection of the most performant AnRes and desorption verification

To evaluate the performances of the three AnRes when actual complex solutions are used, multicomponent adsorption tests were carried out using the pre-treated UBWs1. Hence, three sets of experiments (22 conditions each) were done to define four adsorption isotherms per AnRes, namely: CAs, Cl^-, PO_4^{X-} and COD_{Other}. The 22 experimental points were accomplished according to the general approach described within **Section 2.2**. Therefore, the selectivity of the AnRes towards CAs in the presence of other ions (Cl^-, PO_4^{X-}) and COD_{Other} was evaluated. Importantly, since the observed enrichment factors for each carboxylic acid (defined as EF_j = fraction mol in the resin / fraction mol in solution, where *j* indicates the single acid) were 1-1.2 for the 22 points, overall CA moles were considered to define the CA adsorption isotherms.

After the adsorption test, the vials containing the corresponding AnRes portions with the adsorbed compounds were used to verify the feasibility of applying a simple desorption step, as reported elsewhere [8]. Hence, vials were weighted before and after the addition of NaOH-ethanol solution (3 mL, 0.5 M) to accurately determine the total liquid volume (left liquid plus the added desorbing solution, V_{Des}). After 120 min (at 25°C and 150 rpm), the liquid was separated and analysed for determining desorbed analytes concentrations ($[CAs]_{Des}$, $[Cl^-]_{Des}$, $[PO_4^{x-}]_{Des}$, $[COD_{Other}]_{Des}$). Total desorbed moles were calculated as $C_{Des}.V_{Des}$.

2.2.4. Testing the selected AnRes with different actual broths: matrix influence and calibration of a simple ion equilibrium model

Once the AnRes was selected (**Section 2.2.3**), the other three pre-treated broths (UBWs2, FVWs and GP) were used to define related multicomponent adsorption isotherms by the same experimental procedure described above. This allowed both to *a)* evaluate the resin performance in the treatment of different matrices with different ions mixtures, and *b)* to calibrate a general simplified ion equilibrium model.

2.3. CA adsorption prediction in multicomponent tests based on single component isotherms

Neither the amines (functional group) dissociation nor the other organic compounds (COD_{Other}) occurring in actual broths are as significant as inorganic ions on CA adsorption interference. To confirm this hypothesis, CA adsorption isotherms were initially predicted in all the multicomponent adsorption tests (22 experimental conditions each) conducted with actual broths by considering only: *(i)* the previous obtained Langmuir/Freundlich isotherms for single components tests (acetic acid, Cl^- and PO_4^{x-}, **Section 2.2.1**) and *(ii)* the inorganic ions occurring in the actual broths (Cl^-, PO_4^{x-} and Na^+). Thus, 22 expected isotherms points ($[CAs]_{Eq}$''; q_{Cas}'') were calculated for each multicomponent adsorption tests by following the next rationale (for each experimental point):

1- the overall anion adsorption isotherms ($q_{Tot\ anions}$ *vs* $[Tot\ anions]_{Eq}$) coincides with the same CA isotherm equations (Langmuir or Freundlich, depending on the AnRes) obtained previously using acetic acid prepared solution (**Section 2.2.1**). Thus, an expected equilibrium concentration of overall anions ($[Tot\ anions]_{Eq}$, comprising Cl^-, PO_4^{x-} and CAs) can be calculated from a presumed $q_{Tot\ anions}$ and the corresponding isotherm formula, e.g. $[Tot\_anions]_{Eq} = \left(q_{tot\_anions}/k\right)^{1/n}$ in the case of the Freundlich equation;

2- the moles of Na^+ remained in the effluent after CatRes pre-treatment get paired with the corresponding molar amount of CAs and prevents CA adsorption. Such concentration can be calculated using a charge balance (Eq. S 6 in Sup. Material-Section S3, calculate Na^+_{Tot});

3- the $[Tot\_anions]_{Eq}$ can also be calculated from Eq. 1 (**Section 2.2.1**) by using $C_0 = [Tot\_anions]_0 - Na^+_{Tot}$ and the previous presumed q_{Tot_anions};

4- a true $[Tot\_anions]_{Eq}$ value can be estimated (as well as q_{Tot_anions}) through iterative minimization of the error between both calculated $[Tot\_anions]_{Eq}$ by changing the presumed q_{Tot_anions};

5- considering the stronger affinities of inorganic anions towards the AnRes active sites, the adsorption of CAs takes place (those which are Na^+-free) on vacant exchange sites. Thus, considering total Cl^- and PO_4^{x-} adsorption ($q_{Cl} = [Cl]_0.\frac{V_{Sample}}{m_{res}}$ and $q_{PO_4{}^{x-}} = [PO_4{}^{x-}]_0.\frac{V_{Sample}}{m_{res}}$), the adsorbed CAs can be calculated as $q_{CAs}'' = q_{Tot\_anions} - q_{Cl} - q_{PO_4{}^{x-}}$; and

6- $[CAs]_{Eq}''$ can be calculated using Eq. 1 and the obtained q_{CAs}''.

2.4. Ions equilibriums model

A homogeneous mass action ideal model (type 1) was proposed based on the following equilibrium reactions (equations 2-12), the charge balance (13) and the analytes concentration balances (14-18):

$K_a^{Res} = [ResHOH].[H_3O^+]/[ResH^+]$ (2)

$K_a^{CAs} = [RCOO^-].[H_3O^+]/[RCOOH]$ (3)

$$K_{a1}^{PO_4} = [H_2PO_4^-].[H_3O^+]/[H_3PO_4] \quad (4)$$

$$K_{a2}^{PO_4} = [HPO_4^{2-}].[H_3O^+]/[H_2PO_4^-] \quad (5)$$

$$K_a^{Cl^-} = [Cl^-].[H_3O^+]/[HCl] \quad (6)$$

$$K_a^{Na^+} = [NaOH].[H_3O^+]/[Na^+] \quad (7)$$

$$K_{Res}^{Cl^-} = [ResHCl]/([ResH^+].[Cl^-]) \quad (8)$$

$$K_{Res1}^{PO_4^{x-}} = [ResHH_2PO_4]/([ResH^+].[H_2PO_4^-]) \quad (9)$$

$$K_{Res2}^{PO_4^{x-}} = [(ResH)_2HPO_4]/([ResH^+]^2.[HPO_4^{2-}]) \quad (10)$$

$$K_{Res}^{CAs} = [ResHRCOO]/([ResH^+].[RCOO^-]) \quad (11)$$

$$K_{Na^+}^{CAs} = [NaRCOO]/([Na^+].[RCOO^-]) \quad (12)$$

$$[RCOO^-] + [OH^-] + [H_2PO_4^-] + [HPO_4^{2-}].2 + [Cl^-] = [NH_4^+] + [Na^+] + [H_3O^+] \quad (13)$$

$$Res_{Tot} = [ResH^+] + [ResHOH] + [ResHCl] + [ResHH_2PO_4] + 2.[(ResH)_2HPO_4] + [ResHRCOO] \quad (14)$$

$$CAs_{Tot} = [RCOOH] + [RCOO^-] + [ResHRCOO] + [NaRCOO] \quad (15)$$

$$Cl_{Tot} = [HCl] + [Cl^-] + [ResHCl] \quad (16)$$

$$PO_4^{x-}{}_{Tot} = [H_3PO_4] + [H_2PO_4^-] + [HPO_4^{2-}] + [ResHH_2PO_4] + [(ResH)_2HPO_4] \quad (17)$$

$$Na^+{}_{Tot} = [Na^+] + [NaOH] + [NaRCOO] \quad (18)$$

All concentrations are referred to the total volume of liquid (V_{Tot}), including the free deprotonated ([ResHOH]), free protonated ([$ResH^+$]) and total concentration (Res_{Tot}) of the resin, the latter being calculated as the added quantity of dry resin multiplied by a constant *Q* (moles of active sites per gram of dry resin) and divided by the final volume (V_{Tot}). The proposed homogenous mass action model [16] reflects the following simplifications: *(1)* tertiary and quaternary amines functional groups of the AnRes were considered to have the same average dissociation constant; *(2)* all CAs (acetic, propionic, butyric, valeric, hexanoic acids; with an average K_a of 1.48 x 10^{-5} ± 1.68 x 10^{-6}) have the same dissociation

constant; *(3)* adsorption of sulphates (occurring in traces in the employed broths) was neglected; *(4)* the molar amount of Na^+ still available after the pre-treatment with the CatRes can get paired with the CAs since Na^+ have a higher affinity with carboxylates than the AnRes' exchange sites; *(5)* the low molar amount of Na^+ was not sufficient to consider associations equilibrium reactions for the inorganic anions. Moreover, the mass action model does not consider the calculation of activity coefficients, nor for the liquid phase neither for the solid phase. Instead, these coefficients are included in the resulting equilibrium constants obtained from the calibration.

From all equations (2-18), six final equalities with pH as the only independent variable were used to state a simultaneous equation system, namely: the charge balance and five equations with Langmuir-formula format, one for each of the four anions adsorbed to the resin and one for the CAs paired with the Na^+. Detailed information on these equations were reported in Sup. Material-Section S3.

Importantly, in the case of phosphates, both adsorbed species were added ($[(ResH)_2HPO_4] + [ResHH_2PO_4]$) and considered together for the definition of a total phosphates adsorption isotherm ($q_{PO_4{}^{x-}}$ *vs.* $[PO_4{}^{x-}]_{Eq}$).

As mentioned, the model was calibrated by using four different actual CA-rich broths, i.e. by determining a common value for the constants Q, K_a^{Res}, K_a^{CAs}, $K_{a1}^{PO_4{}^{x-}}$, $K_{a2}^{PO_4{}^{x-}}$, $K_a^{Cl^-}$, $K_a^{Na^+}$, K_w, $K_{Res}^{Cl^-}$, $K_{Res1}^{PO_4{}^{x-}}$, $K_{Res2}^{PO_4{}^{x-}}$, K_{Res}^{CAs} and $K_{Na^+}^{CAs}$ that could describe simultaneously the adsorption on AnRes of target anions occurring in all four effluents. To this aim, a simple MATLAB algorithm was produced. Briefly, it uses the built-in function *patternsearch* to propose a set of guessing values for the constants used in the six pH-dependent equations used in each effluent contemporaneously. Thereafter, the built-in function *fmincon* is used to solve the simultaneous equations at each experimental point of the isotherms with constrains expressed as $[ResHCl] \leq Cl_{Tot}$, $[ResHRCOO] + [NaRCOO] \leq CAs_{Tot}$ and $[ResHH_2PO_4] + [(ResH)_2HPO_4] \leq PO_4{}^{x-}{}_{Tot}$. As a result, modelled bond and free analytes concentrations ($[ResHCl]$,

$[ResHH_2PO_4]$, $[(ResH)_2HPO_4]$, $[ResHRCOO]$, $[NaRCOO]$, $[Cl]_{eq}$, $[{PO_4}^{x-}]_{eq}$, $[CAs]_{eq}$) are estimated for each point of the isotherms by using only the corresponding measured value of pH at equilibrium. Finally, the sum of the weighted square error between the experimental and modelled concentrations is computed as a total of all isotherms for all effluents. This objective function is minimized with the mentioned *patternsearch*. The initial guesses constants values were based on physicochemical known data, namely: resin exchange capacity and affinity-constants observed from the experiments mentioned in **Sections 2.2.1** and **2.2.3**, resin and inorganic ions dissociation constants for diluted systems, and an average CA dissociation constant (mean between all four actual effluent of the composition-weighted-average K_a). The quality of the best fit for each effluent-isotherm and for each compound was evaluated by means of the correlation coefficient $R^2 = 1 - \left[\sum_{i=1}^{22}\left(C_{Exp,i} - C_{Model,i}\right)^2\right] / \left[\sum_{i=1}^{22}\left(C_{Exp,i} - C_{Exp,avg}\right)^2\right]$ and by the residuals $R\% = 100.\left(C_{Exp,i} - C_{Model,i}\right)/C_{Exp,i}$, where $C_{Exp,i}$, $C_{Model,i}$, $C_{Exp,\,Avg}$ are the experimental, modelled and average experimental concentrations values of each compound (Cl^-, ${PO_4}^{x-}$ or CAs), respectively.

2.5. Analytical procedures

CAs, ${PO_4}^{x-}$ and sulphates concentrations were determined by HPLC-RID using the same procedure reported elsewhere [17]. ${NH_4}^+$ and Cl^- concentrations were determined using two combined ion-selective electrodes (ISE) (Crison), while a conventional laboratory probe (XS POLYMER PLAST S7) was used for measuring pH. Resins water content was determined by using a moisture analyser (MB35-OHAUS), which was operated at 105 °C until constant weight was obtained.

Chemical oxygen demand (COD_{Meas}) was determined by using a colorimetric commercial kit (AQUALYTIC Vario MR). This parameter determines the overall concentration of all oxidizable compounds, including the CAs, Cl^- and other organic molecules (COD_{Other}) occurring in each sample. To determine the COD_{Other}, the equivalent COD contributions of CAs and Cl^- were calculated by considering the stoichiometric

oxidation of both (COD_{CAs} and COD_{Cl}, respectively). Thus, the concentration of the matrix compounds was calculated as $COD_{Other} = COD_{Meas} - COD_{CAs} - COD_{Cl}$. Na^+ was determined from the charge balance equation (Sup. Material-Section S3, Eq. S6).

3. RESULTS AND DISCUSSION

3.1. Resin characterization

Single component adsorption isotherms were defined for characterizing the CatRes to be used in the pre-treatment of the four actual broths. **Fig. 1 A** shows the experimental results fitted with Freundlich model for the cases of sodium acetate ($k = 3.97$, $n = 0.13$, $R^2 = 0.95$) and ammonium acetate ($k = 3.55$, $n = 0.141$, $R^2 = 0.94$). Interestingly, Langmuir model resulted less performant in both cases (Sup. Material Fig. S2), but the obtained CatRes maximal exchange capacities for NH_4^+ (q_{max} = 5.30 mmol/$g_{dry\ res}$) and Na^+ (q_{max} = 5.35 mmol/$g_{dry\ res}$) were in accordance with the value estimated using the datasheet (5.4 mmol/$g_{dry\ res}$). Notably, the effectiveness of using the charge balance equation (Eq. S6 in Sup. Material) to determine $[Na^+]_{Eq}$ was indirectly assessed and verified when carrying out the NH_4^+ adsorption isotherm test. Indeed, the comparison between the ISE measured values of $[NH_4^+]_{Eq}$ (**Section 2.5**) with those obtained by using Eq. S6 (and the corresponding pH values at the equilibrium) showed high correspondence in a parity plot (Sup. Material Section S2.3, Fig. S3).

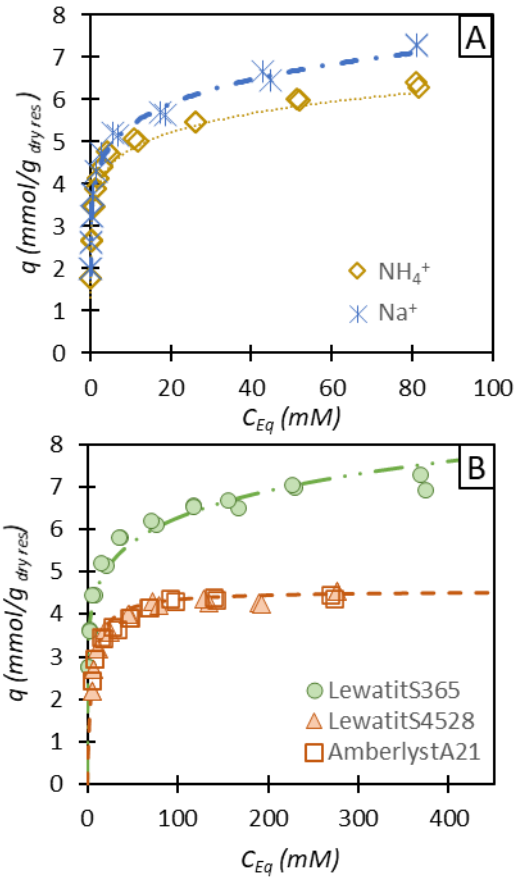

Fig. 1: Resin characterization: Na^+ and NH_4^+ adsorption isotherms with the CatRes Lewatit S2568H (A) and acetic acid adsorption with the three AnRes (B). For the isotherm profiles, markers represent the experimental results whereas lines refer to fittings of Langmuir or Freundlich isotherms. A single modelled curve is presented for acetic acid adsorption onto both tertiary amine resins.

As for the AnRes, **Fig. 1 B** shows examples of acetic acid adsorption isotherms for the three AnRes tested in this work. Lewatit A365 isotherms have Freundlich behaviours (shown in **Fig. 1 B**), as typical for bifunctional/heterogenous resins [18], with the highest affinity for Cl^- ($k = 7.59$, $n = 0.08$, $R^2 = 0.93$),

followed by PO_4^{x-} ($k = 5.79$, $n = 0.13$, $R^2 = 0.89$) and CAs ($k = 3.51$, $n = 0.126$, $R^2 = 0.94$). Conversely, both resins with tertiary amine have extremely similar Langmuir behaviours, e.g. isotherms parameter for CAs were $q_{CAs,max} = 4.54\, mmol/g_{dry\,res}$, $K_s = 4.74\, mM$, $R^2 = 0.90$, and the same order of affinities previously found for the bifunctional resin was observed (Cl^- > PO_4^{x-} > CAs). The obtained results confirm the higher exchange capacity of the bifunctional resin over the others AnRes: Lewatit A365 has a remarkable 1.56 folds increase of the CA adsorption capacity of Lewatit S4528 or Amberlyst A21, the last one previously proposed by a study addressed to the same purpose [8].

Furthermore, coupling the adsorption of nutrients such as NH_4^+ and PO_4^{x-} to CA extraction is of interest in the perspective of maximizing resource recovery from waste and by-products; this approach might represent an improvement towards the entire process sustainability [19,20]. The results obtained with the CatRes reveal that Na^+ and NH_4^+ have similar affinities with the solid phase, while the results attained with the anionic resins suggest that single anions recovery could be accomplished by splitting the AnRes step in three dedicated columns addressed to the extraction of Cl^-, PO_4^{x-} and CAs, respectively.

3.2. Actual broth pre-treatments with cationic resin

The feasibility of recovering CAs by employing sequentially cationic and anionic resins was verified with four actual effluents. To this aim, the UBWs1, UBWs2, FVWs and GP broths were treated with the CatRes as described in **Section 2.2.2**. While the contents of CAs, inorganic anions and total COD remained almost unaltered (ca. 90%), the pH dropped since cations were removed and CAs remained as acids (**Table 1**). Moderate to low adsorption of COD_{Other} by the CatRes was observed in all pre-treatments (< 50%), in accordance with previously reported statements for the treatment of corn stover hydrolysate with another strong CatRes [21]. The pre-treatment of UBWs1, FVWs and GP broths for obtaining cation-free effluents required the implementation of seven adsorption-desorption cycles in 60 mL packed syringe. Although those cycles were not conducted as breakthrough tests, the CatRes reusability was preliminary

assessed when treating the UBWs2 at pilot scale by performing five breakthrough test and desorption cycles (data not shown). The obtained exchange capacity repeatability and low deviations (5.10 ± 0.53 $mmol/g_{dry\ res}$) can be considered a preliminary promising result which must be confirmed by applying several cycles at pilot scale.

The effectiveness of the pre-treatments paves the way for future investigation about cation adsorption isotherms using actual effluents in order to model also this step using ion equilibrium and to better refine the overall two stage process. However, the present work was focused on the recovery of the CAs, which were demonstrated to be inert to the CatRes step.

Table 1: CA-rich effluents features before (pre) and after (post) their treatment with the CatRes Lewatit S2568H

Effluent	COD_{Meas} (mM O_2) [a]	CAs (mM) [a]	Cl^- (mM) [a]	PO_4^{x-} (mM) [a]	COD_{Other} (mM O_2) [d]	pH [a]	NH_4^+ (mM) [a]	Na^+ (mM) [b, d]	μ [c] (mM) [d]
UBWs1-*pre*	1509 ± 26	289 ± 10	44.5 ± 2.1	11.0 ± 0.8	576 ± 50	5.75 ± 0.01	38.36 ± 2.91	279.92 ± 14.92	318.54 + 14.95
UBWs1-*post*	1350 ± 24	276 ± 7	41.1 ± 3.1	9.5 ± 0.4	398 ± 50	1.51 ± 0.01	0.96 ± 0.29	11.39 ± 3.47	27.79 ± 3.47
UBWs2-*pre*	2078 ± 200	348 ± 2	44.0 ± 2.8	5.8 ± 0.2	683 ± 206	5.75 ± 0.01	34.78 ± 2.06	323.61 ± 6.88	358.58 ± 6.89
UBWs2-*post*	1598 ± 14	345 ± 3	36.0 ± 5.6	5.8 ± 0.5	372 ± 24	1.46 ± 0.01	0.23 ± 0.09	2.30 ± 5.78	19.86 ± 5.78
FVWs-*pre*	1256 ± 39	283 ± 1	23.4 ± 1.4	0.1 ± 0.1	162 ± 45	7.00 ± 0.01	37.93 ± 1.91	266.76 ± 4.43	304.50 ± 4.47
FVWs-*post*	1261 ± 40	275 ± 3	21.7 ± 2.8	0.1 ± 0.1	259 ± 50	1.80± 0.01	0.72 ± 0.23	5.44 ± 3.07	14.08 ± 3.07
GP-*pre*	977 ± 63	230 ± 8	26.0 ± 0.4	8.1 ± 0.3	159 ± 90	7.05 ± 0.01	5.44 ± 0.52	313.31 ± 9.30	322.17 ± 9.42
GP-*post*	962 ± 48	221 ± 4	24.3 ± 1.9	8.3 ± 0.4	191 ± 59	2.44 ± 0.01	0.83 ± 0.11	26.41 ± 2.30	29.09 ± 2.30

[a] errors from analytical determination; [b] calculated by charge balance (Supplementary material Eq. S 6), by using the concentration of CAs, Cl^-, PO_4^{x-} and NH_4^+ previously determined; [c] approximate ionic strength calculated as reported elsewhere [22] by considering CAs (i.e. $R\text{-}COO^-$), Cl^-, PO_4^{x-}, NH_4^+ and Na^+; [d] errors calculated by error propagation.

3.3. Selection of the most performant AnRes and desorption verification

For comparing the three AnRes performances, multicomponent adsorption tests were carried out using the pre-treated UBWs1. **Fig. 2 A, B and C** show the competitive adsorption of CAs, Cl^-, PO_4^{x-} for each AnRes. Complementarily, **Fig. 2 D, E and F** expose (for the same batch tests) the competitive adsorption in

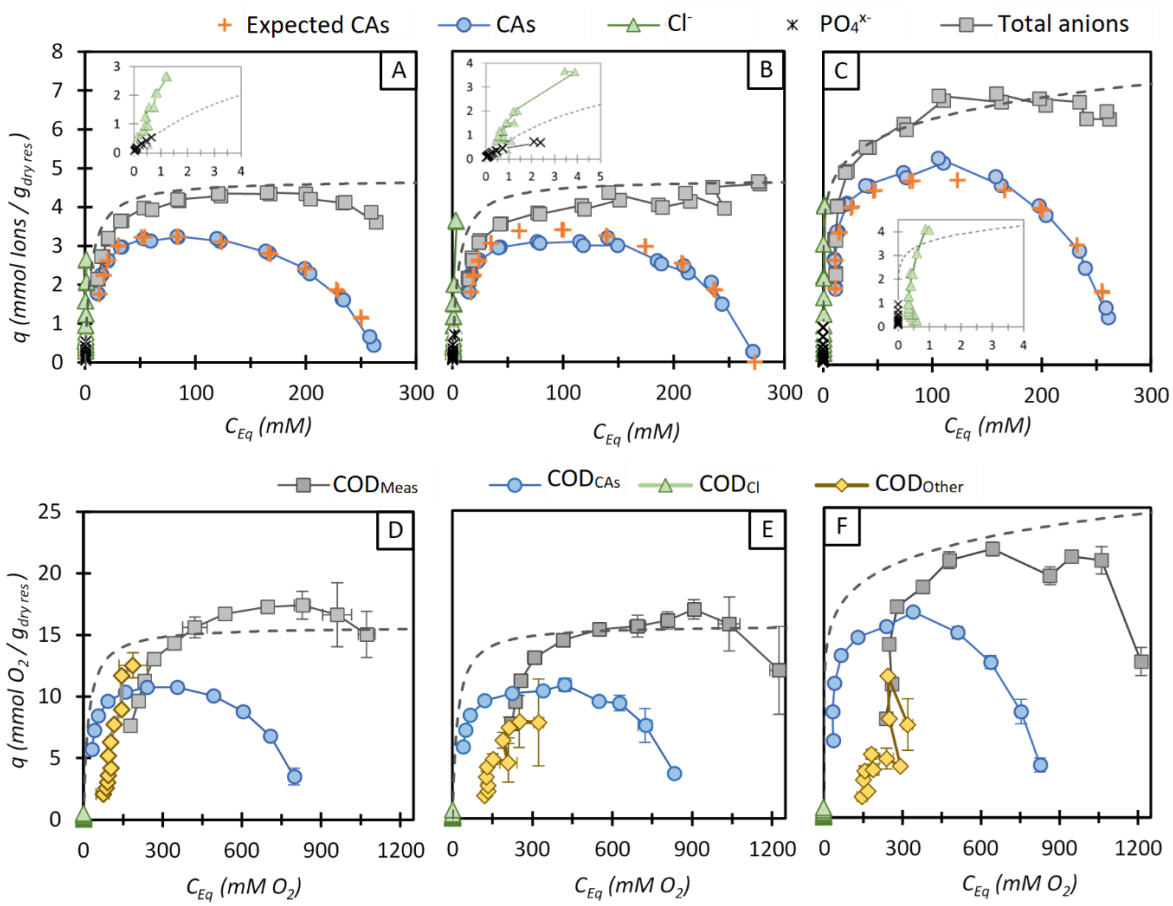

Fig. 2: Multicomponent competitive adsorption batch tests performed using UBWs1 and the AnRes Amberlyst A21 (A & D), Lewatit S4528 (B & E) and Lewatit A365 (C & F). Adsorption experimental trends (markers with lines) in terms of anions (A, B, C) and in terms of COD (D, E, F). For comparison, predicted CA adsorption points (+) were presented as well as the corresponding acetic acid isotherms (Langmuir or Freundlich) obtained from the single component tests (dashed lines).

terms of COD_{CAs}, COD_{Cl} and COD_{Other}. The experimental points representing the adsorption of total anions (**Fig. 2 A, B and C**) had similar profiles with respect to those previously obtained with acetic acid (dotted line), while the CA isotherms followed bell-shaped trends. In fact, at low liquid to resin ratios (C_{Eq} < 50 mM) almost all anions were adsorbed, while at higher ratios the resin underwent saturation (i.e. all exchange sites are bound to an anion). When saturated (C_{Eq} > 120 mM), the CA adsorption decreased since the AnRes sites have a higher affinity with the inorganic anions (Cl^- or PO_4^{x-}). Indeed, expected CA adsorption points were predicted by considering the acetic acid isotherms previously obtained in **Section**

2.2.1 along with the inorganic cations and anions interferences (rational in **Section 2.2.4**). The expected points ($[CAs]_{Eq}$''; q_{CAs}'') resulted quite accurate as shown in **Fig. 2** (marker +), with correlation coefficients (R^2) of 0.93 (Amberlyst A21), 0.92 (Lewatit S4528) and 0.95 (Lewatit A365). Contrary to what reported elsewhere [8], such an accurate prediction suggests that the adsorption of COD_{Other} (**Fig. 2 D, E and F**) did not significantly interfere with CA adsorption mechanism. Therefore, either COD_{Other} affinity is lower than that of CAs or its adsorption is due to physisorption (i.e. without occupying exchange sites). The obtained results suggest that the key concern is to separate Na^+ as much as possible before applying the anion adsorption step, rather than optimizing the AnRes protonation by adding inorganic anions. The higher affinity of Cl^- and PO_4^{x-} was confirmed for all AnRes. Indeed, it was not possible to measure the $[PO_4^{x-}]_{Eq}$ for the bifunctional resin (Lewatit A365) case, probably due to the higher affinity and capacity of this AnRes.

The resulting CA adsorption isotherms, shown in **Fig. 2 A, B and C**, confirmed the improvement obtained by the application of the proposed strategy. The resins with tertiary amines adsorbed ca. 3.2 mmol/$g_{dry\ res}$ of CAs (**Fig. 2 A and B**); notably, this value is more than 2 times higher than the one reported by [8] for the same Amberlyst A21. Indeed, the UBWs1 employed was almost free of cations while the actual broth used in the cited work contained almost equimolar quantities of Na^+ and CAs. The bifunctional resin (Lewatit A365) exerted a CA adsorption capacity even higher: up to 5.3 mmol CAs/$g_{dry\ res}$ were extracted (**Fig. 2 C**), thus this adsorbent was selected for the consecutive experiments.

Regarding the desorption, the obtained results (shown in **Fig. 3 A and B**) confirmed the feasibility of using a NaOH-Ethanol solution (0.5 M), in agreement with previous evidences [8]. All resins showed almost perfect correspondence between total desorbed CAs or overall COD and the previously adsorbed amounts (on mmol bases). Small deviations from the linear relation were obtained for the conditions containing low amounts of resin, ascribed to the inherent analytical procedures accuracy for determining the q_{CAs} at those conditions. Moreover, results presented in **Fig. 3 B** allowed inferring that also COD_{Other}

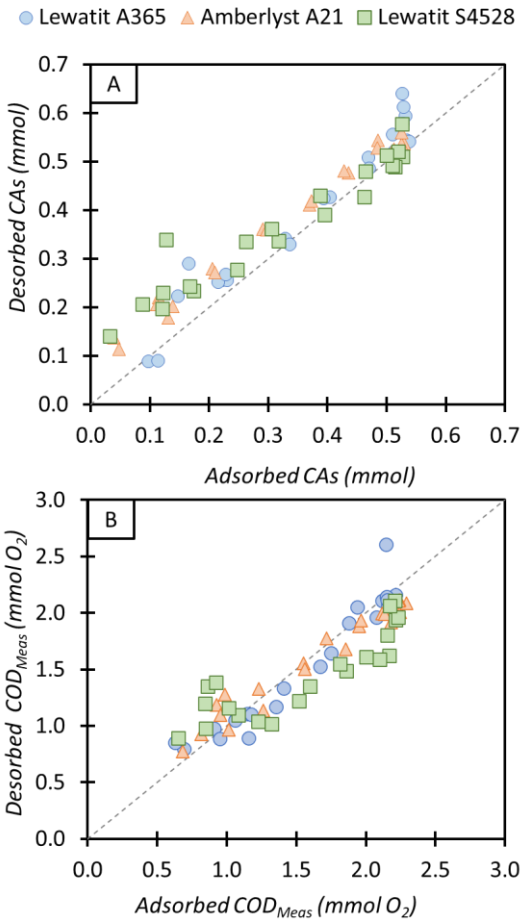

Fig. 3: Desorption tests using NaOH-ethanol solution and the AnRes portions belonging to the previous multicomponent adsorption tests with UBWs1. Total moles desorbed *vs.* total moles previously adsorbed regarding CAs (A) and COD_{Meas} (B).

and Cl^- were desorbed. Regarding PO_4^{x-} desorption, due to its low concentration, it was not possible to accurately determine its titer in the desorption solutions. Notwithstanding this, complete desorption of phosphates was assumed, in accordance with their lower affinity (with AnRes) than that of Cl^- ions, which were completely desorbed as previously mentioned. With all this in mind, and since the desorption step was verified to be a feasible and effective process, the following research activities were focused on the adsorption step.

3.4. Testing the selected AnRes with different actual broths: matrix influence and calibration of a simple ion equilibrium model

To assess the actual broths matrix effects on the performance of Lewatit S365, three more multicomponent competitive adsorption tests were performed using the pre-treated UBWs2, FVWs and GP. The obtained adsorption isotherms are shown in **Fig. 4 A-D**, also including UBWs1 profiles (**Fig. 2 C**) for comparison. CA isotherms resulted to have bell-shaped trends for these actual broths as well. They were accurately predicted by the expected CA adsorption points ($[CAs]_{Eq}$''; q_{CAs}'') as indicated by the obtained correlation coefficients (R^2): 0.90 (UBWs2), 0.90 (FVWs) and 0.94 (GP). Besides, these high correspondences confirmed that the single organic acids occurring in the broths have similar affinities for the AnRes since the method for predicting the CA adsorption points considered the overall CA mole concentration (**Section 2.3**). In agreement with this, the enrichment factors of each adsorbed acid (EF_j) resulted 1-1.2 for all experimental conditions tested (22 for each broth). All maximal values of q_{CAs} indicated that more than 84% of the resin exchange capacity was utilized for adsorbing CAs. Even in the case of the GP broth, containing the highest concentration of Na^+ (pH 2.43), about 70% of the AnRes exchange sites were engaged by CAs. Moreover, as formerly observed for UBWs1, the related low phosphates concentration occurring in UBWs2, FVWs and GP did not allow to determine PO_4^{x-} concentration in the liquid phase at the equilibrium.

A simplified mass action ideal model was proposed for predicting anions adsorption isotherms. Differently from the model previously proposed elsewhere [8], it considered the competitive effects of the anions (CAs, Cl^- and PO_4^{x-}) and cations (Na^+) naturally occurring in the broths. The model was calibrated by using the multicomponent adsorption results obtained with the four actual broths. The Matlab-function *patternsearch* obtained the best fitting values of the unknow parameters after 50-100 function

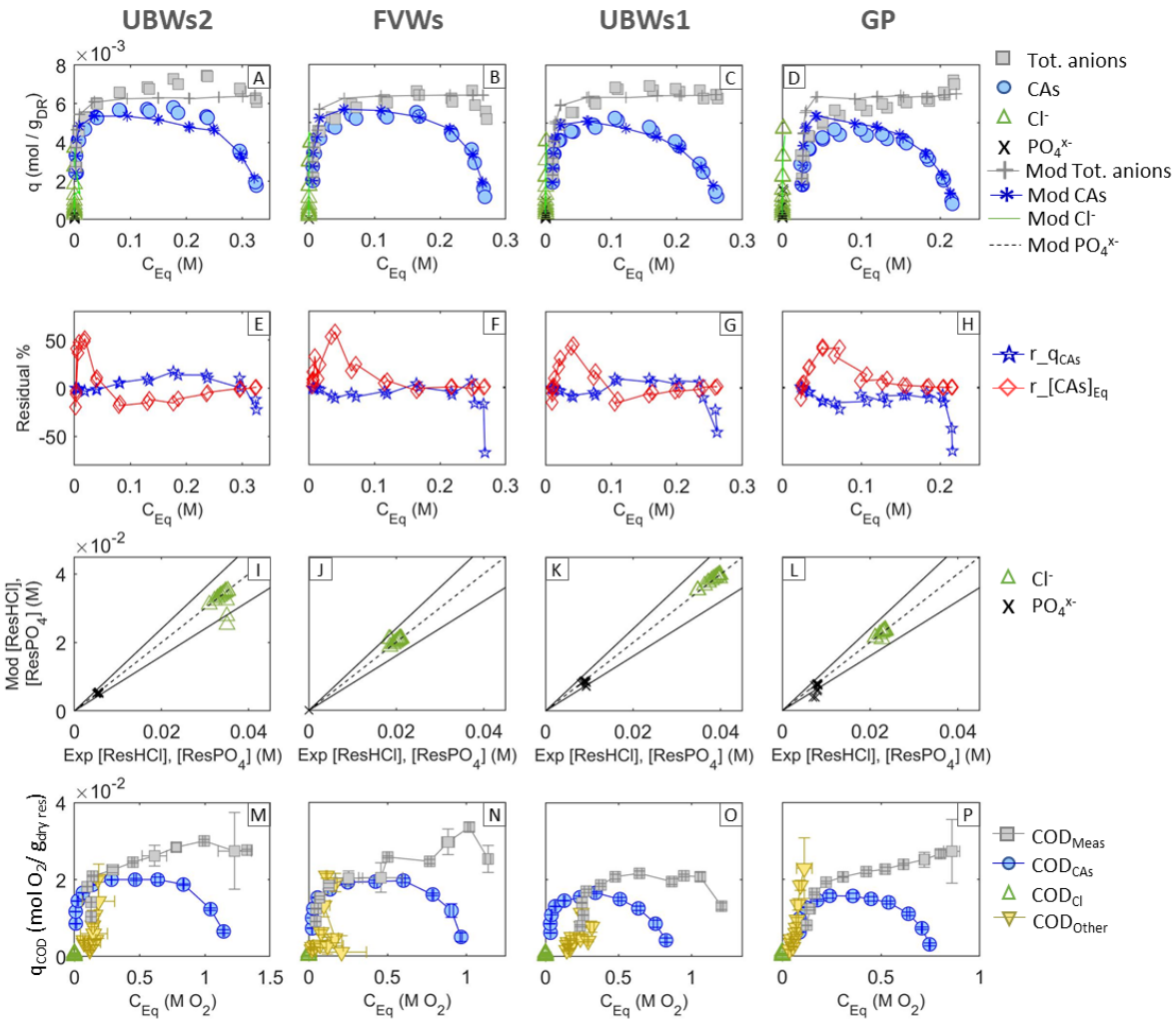

Fig. 4: Multicomponent competitive adsorption tests performed using the Lewatit A365 and the actual effluents UBWs2 (A, E, I, M), FVWs (B, F, J, N), UBWs1 (C, G, K, O) and GP (D, H, L, P). First row of graphics shows adsorption experimental trends (markers) as well as modelled points (markers with line, e.g. Mod CAs) using the ions equilibrium model. Second graphics row shows q_{CAs} and $[CAs]_{Eq}$ residuals (r). Third row shows experimental vs. modelled parity plots (±20%) for adsorbed Cl^- and PO_4^{X-}. Last row shows the averaged adsorption experimental trends in terms of COD.

evaluations, namely (initial values): $Q = 6.767 \times 10^{-3}\, mol/g_{dry\,res}$ (7.5x10^{-3}), $K_a^{Res} = 9.9999 \times 10^{-14}$ (1×10^{-13}), $K_a^{CAs} = 1.4427 \times 10^{-5}$ (1.545×10^{-5}), $K_{a1}^{PO_4^{x-}} = 7.2608 \times 10^{-3}$ (7.11×10^{-3}), $K_{a2}^{PO_4^{x-}} = 6.3768 \times 10^{-8}$ (6.32×10^{-8}), $K_a^{Cl^-} = 1.3317 \times 10^{6}$ (1.2589×10^{6}), $K_a^{Na^+} = 1.0003 \times 10^{-15}$ (1×10^{-14}), $K_w = 1.0836 \times 10^{-14}$ (1×10^{-14}), $K_{Res}^{Cl^-} = 8.1440 \times 10^{4}$ (8×10^{4}), $K_{Res1}^{PO_4^{x-}} =$

5.7766×10^3 (6×10^3), $K_{Res2}^{PO_4^{x-}} = 7.4879 \times 10^4$ (7×10^4), $K_{Res}^{CAs} = 5.1651 \times 10^3$($5 \times 10^3$) and $K_{Na^+}^{CAs} = 1.0766 \times 10^6$ (1×10^6), with an objective function error of ca. 15 (initially being ca. 40). The best estimate of the Lewatit A365 exchange capacity (Q) resulted to be in accordance with the average free CA content in the four effluents (ca. 265 mM, representing ca. 90% of total anions) and with the acetic acid isotherm presented in the previous **Section 3.1** ($3.51 \times 265^{0.126} = 7.09 \times 10^{-3}\, mol/g_{dry\ res}$). The estimated dissociation constants (K_a for the inorganic acids and bases, respectively) resulted slightly higher than the standard constants for diluted systems (here used as initial guessing values), this in accordance with the electrolytes concentration effects [22]. As shown in **Table 2** and **Fig. 4 E, F, G and H** the proposed pH-dependent model allows a very good overall fit of the experimental CA concentrations in the liquid phase ($[CAs]_{Eq}$) and in the solid phase ([ResHRCOO] and q_{CAs}), even at higher Na^+ concentration, as in GP broth. Considering the residual trends shown in these graphics, it can be observed that the proposed model is characterised by a good prediction of: *(i)* the CA concentrations in the solid ([ResHRCOO]) excepting for the last point/s at the lowest amounts of AnRes; *(ii)* the liquid total CA concentrations ($[CAs]_{Eq}$) for values ≥ 0.1 M (errors <20%), while higher errors were detected (up to 50%) at lower concentrations as previously reported elsewhere [8]. However, in the present work such deviations are not only ascribed to low intrinsic accuracy of the HPLC-RID analyses at low CA concentrations but also to the likely existence of an inflexion point difficult to be accurately predicted by this model. This is evident when observing the GP's residual curve for $[CAs]_{Eq}$ (**Fig. 4 H**, diamond marker), whose maximum value corresponds to a higher $[CAs]_{Eq}$ than those of other effluents. Regarding the accuracy for inorganic anions, the low liquid concentrations at the equilibrium for Cl^- and the inability to detect PO_4^{x-} forced to analyse the model performance in terms of the adsorbed concentrations prediction (**Fig. 4 I, J, K and L**). Few points of chloride and phosphates curves did not perfectly fit with the model, this was ascribed to the lack of precision when analytes with high affinities for the AnRes occurred at very low

concentration. Despite this, good correlation values were obtained for q_{Cl^-} and $q_{PO_4{}^{x-}}$ (**Table *2***). The concordance of prediction capacity among different effluents confirms the model is dependable.

Table 2: Fitting quality of the proposed model with the different effluents in terms of correlation coefficients (R^2) for the solid and liquid concentrations

EFFLUENT	$R^2_{[ResHRCOO]}$	$R^2_{q_{CAs}}$	$R^2_{[CAs]_{Eq}}$	$R^2_{q_{Cl^-}}$	$R^2_{q_{PO_4}}$
UBWS2	0.99	0.90	0.99	0.98	0.98
FVWS	0.99	0.95	0.99	0.98	0.96
UBWS1	0.99	0.94	0.99	0.99	0.93
GP	0.96	0.88	0.97	0.99	0.84

Concerning the AnRes selectivity, COD_{Other} was adsorbed in all effluents (**Fig. 4 M, N, O and P**). Yet, the expected CA isotherms (q_{CAs}'' vs. $[CAs]_{Eq}$'') and the ion equilibrium model both accurately predicted the CA adsorption quantities even when calculations did not consider COD_{Other}. This evidence suggests the occurrence of COD_{Other} physisorption rather than ionic sorption. Sure enough, even if driven by chemisorption, its affinity is lower than that of CAs, since all the COD_{Other} isotherms are positioned at the right of the bell-shaped COD_{CAs} isotherms. The only exception was the one of GP broth, where the higher Na^+ content (higher pH) made the bell-shape "translation" to the right while the COD_{Other} affinity remained invariable.

All the obtained results showed that the separation of the Na^+ before recovering CAs by employing an AnRes is crucial. Indeed, *Zeidan and Marti* observed almost identical trends of formic acid adsorption efficiency vs. initial effluent pH when using Amberlite IRA 96 (with tertiary amines) or Lewatit MP 64 (with tertiary and quaternary amines), this meaning that the strong basic quaternary amines resulted to have the same efficiency of a weak basic resin which is not always completely dissociated [23]. Moreover, **Fig.**

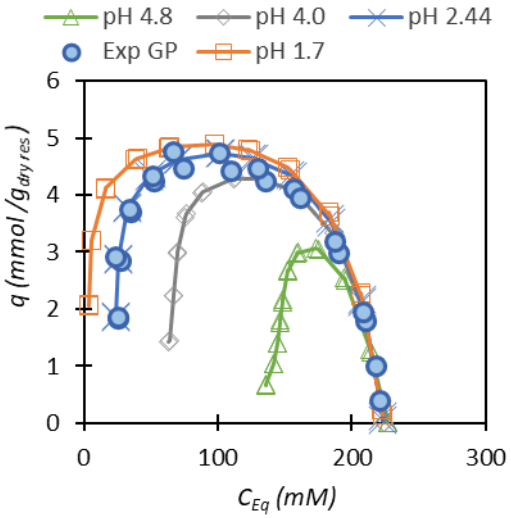

Fig. 5: Effect of GP's Na^+-content on the resulting CA isotherms. Simulated curves using the same portions and GP broth compositions belonging to the results shown in Fig.4 except for the different Na^+ contents represented by different initial pH. For comparison, experimental CA adsorption points obtained using the actual GP at its initial pH of 2.43 were also plot.

5 illustrates how Na^+ content (inferable by the effluent's initial pH) would affect the GP's CA-isotherms. Four expected CA isotherms were simulated by considering the implementation of the same AnRes portions and GP broth composition used in the previous experiment, but with different Na^+ concentrations and thus with the following pH values: 1.7, 2.4 (verified experimental condition), 4.0 and 4.9. It is an advantage to obtain "favourable" CA adsorption isotherms, i.e. the closer the curve to the *q* axis the higher the amount of CAs potentially recovered. This can be figured out when considering process operating lines and equilibriums for the adsorption equipment design [24].

It is well known that repeated adsorption-desorption cycles should be carried out to verify the resin reutilization. Hence, a preliminary test was carried out in the present work by performing three consecutive cycles using the UBWs2, the AnRes Lewatit A365 and the same 10 mL vial previously employed. In addition to the desorption carried out with the NaOH solution (also serving to resin regeneration), a water washing step was added. The CA adsorption yielded on average 5.67 mmol/$g_{dry\ res}$ (± 11.7%), while the desorption yielded 0.95-1.09 mmol of desorbed CAs per mmol of adsorbed CAs. As a whole, the proposal resulted technically feasible and effectively improved the CA recovery using a weak AnRes (with high exchange capacity). Notably, the assessed mass action ideal model considers the interferences from Cl^-, PO_4^{x-} and Na^+ occurring in typical CA-rich effluents and it is not affected by matrix effects due to type and concentration of undefined compounds occurring in different broths (COD_{Other}). The model turned out to be accurate for the prediction of various experimental conditions, including different ionic strength conditions along an isotherm and even the employment of very dissimilar broths with different type and concentrations of: matrix contained compounds (COD_{Other}, 191-398 mM O_2), CAs (221-348 mM), Na^+ (pH 1.5-2.43, i.e. 6.4-27.2 mM), PO_4^{x-} (0.1-9.5 mM) and Cl^- (21.7-41.1 mM). Regarding the use of concentration equilibrium constants, the obtained accuracy is still justified by the facts that ionic strengths of CA-rich broths were not significantly high (14-29 mM). Thus, exerting low electrolyte effects, e.g.: limited variations of 7% and 8% with respect to the thermodynamic constants of K_a^{CAs} and K_w were observed. Besides, among potential species that could exert higher electrolyte effects (PO_4^{-2} and SO_4^{-2}), only PO_4^{-2} slightly occurred in the tested broths. Of course, if required, more accurate fittings can be obtained by performing calibrations for each effluent or by using thermodynamic constants and activity coefficients. However, the purpose of the present work was to adjust a unique simplified model capable of predicting the adsorption isotherms despite working with different effluents and compositions. This can represent an effective tool e.g. *i)* when designing such a recovery process since there would be

no need to dispose of representative experimental adsorption isotherms for a specific effluent, or *ii)* to monitor batch adsorption processes by using only a pH-meter.

Results are very encouraging in the perspective of scaling up and optimizing the process at pilot scale, in order to target effective CA extractions for many potential applications in the framework of the carboxylate platform. In this regard, adsorption processes at industrial scale are typically run under semi continuous conditions, i.e. columns are set-up in pairs where alternately one operates in adsorption and the other in desorption modes. Therefore, future pilot-scale studies should include (for both cationic and anionic resins) *i)* adsorption break-through tests at different feeding rates using an actual CA-rich stream and *ii)* desorption tests. These studies would allow to: *1)* construct curves defining the adsorption capacity utilization yield vs feeding rate; *2)* verify and optimize desorption procedures; *3)* evaluate the repeatability of both resin exchange capacities by the application of a significative number of cycles, including the assessment of resin contamination as well as dedicated regeneration steps for decontamination; and, finally, *4)* evaluate the process overall economic feasibility.

4. Conclusions

The application of a cationic resin step for adsorbing Na^+ before applying an anionic resin adsorption step for recovering CAs from fermentation broths highly improved the CA-capture performance. Obtained recovery yields from actual broths resulted over two folds higher than previously reported values.

The proposed calculation-receipt for predicting the CA adsorption isotherms in multicomponent competitive system demonstrated to be an accurate and simple tool for designing adsorption tests. The proposed homogeneous mass action ideal model showed a very good capability to predict multicomponent competitive adsorption isotherms at different conventional process conditions.

Interferences from Cl^-, PO_4^{x-} and Na^+ occurring in typical CA-rich broths resulted more significant than

interferences due to the adsorption of other organic compounds or than the optimization of anionic resins dissociation previously reported in the literature.

Declaration of Competing Interest

The authors declare that they have no known competing financial interests or personal relationships that could have appeared to influence the work reported in this paper.

Acknowledgements

The research received financial support by EU Horizon 2020 Work Programme 2016 – 2017 project ResUrbis ("*RESources from URban BIo-waSte*"). The authors would like to acknowledge Prof. Krzysztof Kolodziejczyk, for his collaboration in the frame of Weronica's internship.

5. References

[1] M.T. Agler, B.A. Wrenn, S.H. Zinder, L.T. Angenent, Waste to bioproduct conversion with undefined mixed cultures: the carboxylate platform, Trends Biotechnol. 29 (2011) 70–78. doi:10.1016/j.tibtech.2010.11.006.

[2] C.S. López Garzón, A.J.J. Straathof, Recovery of carboxylic acids produced by fermentation., Biotechnol. Adv. 32 (2014) 873–904. doi:10.1016/j.biotechadv.2014.04.002.

[3] EU Project-RES URBIS, Resources from Urban Biowaste, EU H2020. (2020). https://www.resurbis.eu/ (accessed March 18, 2020).

[4] G. Moretto, I. Russo, D. Bolzonella, P. Pavan, M. Majone, F. Valentino, An urban biorefinery for food waste and biological sludge conversion into polyhydroxyalkanoates and biogas, Water Res. 170 (2020) 115371. doi:https://doi.org/10.1016/j.watres.2019.115371.

[5] L. di Bitonto, S. Menegatti, C. Pastore, Process intensification for the production of the ethyl esters of volatile fatty acids using aluminium chloride hexahydrate as a catalyst, J. Clean. Prod. 239 (2019) 118122. doi:https://doi.org/10.1016/j.jclepro.2019.118122.

[6] C.I. Cabrera-Rodríguez, C.M. Cartin-Caballero, E. Platarou, F.A. de Weerd, L.A.M. van der Wielen, A.J.J. Straathof, Recovery of acetate by anion exchange with consecutive CO2-expanded methanol desorption: A model-based approach, Sep. Purif. Technol. 203 (2018) 56–65. doi:https://doi.org/10.1016/j.seppur.2018.03.068.

[7] H. Uslu, Adsorption equilibria of formic acid by weakly basic adsorbent Amberlite IRA-67: Equilibrium, kinetics, thermodynamic, Chem. Eng. J. 155 (2009) 320–325. doi:https://doi.org/10.1016/j.cej.2009.06.040.

[8] S. Rebecchi, D. Pinelli, L. Bertin, F. Zama, F. Fava, D. Frascari, Volatile fatty acids recovery from the effluent of an acidogenic digestion process fed with grape pomace by adsorption on ion exchange resins, Chem. Eng. J. 306 (2016) 629–639. doi:10.1016/J.CEJ.2016.07.101.

[9] M.A. Mehablia, D.C. Shallcross, G.W. Stevens, Prediction of multicomponent ion exchange equilibria, Chem. Eng. Sci. 49 (1994) 2277–2286. doi:https://doi.org/10.1016/0009-2509(94)E0041-N.

[10] L.A. Tung, C.J. King, Sorption and extraction of lactic and succinic acids at pH > pKa1. I. Factors governing equilibria, Ind. Eng. Chem. Res. 33 (1994) 3217–3223. doi:10.1021/ie00036a041.

[11] Z. Sheng, B. Tingting, C. Xuanying, W. Xiangxiang, L. Mengdi, Separation of Succinic Acid from Aqueous Solution by Macroporous Resin Adsorption, J. Chem. Eng. Data. 61 (2016) 856–864. doi:10.1021/acs.jced.5b00713.

[12] M.I. González, S. Álvarez, F.A. Riera, R. Álvarez, Purification of Lactic Acid from Fermentation Broths by Ion-Exchange Resins, Ind. Eng. Chem. Res. 45 (2006) 3243–3247. doi:10.1021/ie051263a.

[13] D. KON, Adriaan, A.B. DE HAAN, J. VAN DER WEIDE, Paulus, Loduvicus, T. ĐEKIC ŽIVKOVIC, J. DE KONINCK, Lucien, Henri, Leander, CARBOXYLIC ACID RECOVERY FROM MAGNESIUM CARBOXYLATE MIXTURE, WO2013174911, 2013. https://patentscope.wipo.int/search/en/detail.jsf?docId=WO2013174911&tab=PCTBIBLIO (accessed March 28, 2020).

[14] N.A.M. Zaini, A. Chatzifragkou, V. Tverezovskiy, D. Charalampopoulos, Purification and polymerisation of microbial d-lactic acid from DDGS hydrolysates fermentation, Biochem. Eng. J. 150 (2019) 107265. doi:https://doi.org/10.1016/j.bej.2019.107265.

[15] S.M. Husson, C.J. King, Multiple-Acid Equilibria in Adsorption of Carboxylic Acids from Dilute Aqueous Solution, Ind. Eng. Chem. Res. 38 (1999) 502–511. doi:10.1021/ie9804430.

[16] P.F. Lito, S.P. Cardoso, J.M. Loureiro, C.M. Silva, Ion Exchange Equilibria and Kinetics BT - Ion Exchange Technology I: Theory and Materials, in: I. Dr., M. Luqman (Eds.), Springer Netherlands, Dordrecht, 2012: pp. 51–120. doi:10.1007/978-94-007-1700-8_3.

[17] G.A. Martinez, S. Rebecchi, D. Decorti, J.M.B. Domingos, A. Natolino, D. Del Rio, L. Bertin, C. Da Porto, F. Fava, Towards multi-purpose biorefinery platforms for the valorisation of red grape pomace: production of polyphenols, volatile fatty acids, polyhydroxyalkanoates and biogas, Green Chem. 18 (2016) 261–270. doi:10.1039/C5GC01558H.

[18] M.Z. Southard, D.W. Green, Perry's Chemical Engineers' Handbook, 9th Edition, McGraw-Hill Education, 2018. https://books.google.it/books?id=eW5eswEACAAJ.

[19] H. Bacelo, A.M.A. Pintor, S.C.R. Santos, R.A.R. Boaventura, C.M.S. Botelho, Performance and prospects of different adsorbents for phosphorus uptake and recovery from water, Chem. Eng. J. 381 (2020) 122566. doi:https://doi.org/10.1016/j.cej.2019.122566.

[20] H. Gong, Z. Wang, X. Zhang, Z. Jin, C. Wang, L. Zhang, K. Wang, Organics and nitrogen recovery from sewage via membrane-based pre-concentration combined with ion exchange process, Chem. Eng. J. 311 (2017) 13–19. doi:https://doi.org/10.1016/j.cej.2016.11.068.

[21] E.M. Karp, R.M. Cywar, L.P. Manker, P.O. Saboe, C.T. Nimlos, D. Salvachúa, X. Wang, B.A. Black, M.L. Reed, W.E. Michener, N.A. Rorrer, G.T. Beckham, Post-Fermentation Recovery of Biobased Carboxylic Acids, ACS Sustain. Chem. Eng. 6 (2018) 15273–15283. doi:10.1021/acssuschemeng.8b03703.

[22] D.A. Skoog, D.M. West, F.J. Holler, S.R. Crouch, Fundamentals of Analytical Chemistry, Cengage Learning, 2013. https://books.google.it/books?id=8bIWAAAAQBAJ.

[23] H. Zeidan, M.E. Marti, Separation of Formic Acid from Aqueous Solutions onto Anion Exchange Resins: Equilibrium, Kinetic, and Thermodynamic Data, J. Chem. Eng. Data. 64 (2019) 2718–2727. doi:10.1021/acs.jced.9b00128.

[24] R.E. Treybal, Mass-transfer Operations, McGraw-Hill, 1980. https://books.google.it/books?id=s4RKAQAACAAJ.